Preprint of the paper

"SPH approaches for free surface flow for engineering applications"
G. Mosqueira, L. Cueto-Felgueroso, I. Colominas, F. Navarrina, M. Casteleiro (2002)
Proceedings del "V World Congress on Computational Mechanics" (en Internet).
Viena, Austria.

WCCM V
Fifth World Congress on
Computational Mechanics
July 7–12, 2002, Vienna, Austria
Eds.: H.A. Mang, F.G. Rammerstorfer,
J. Eberhardsteiner

SPH approaches for free surface flows in engineering applications

G. Mosqueira, L. Cueto-Felgueroso, I. Colominas, F. Navarrina and M. Casteleiro*

Group of Numerical Methods in Engineering, GMNI
Civil Engineering School, University of Corunna,
Campus de Elviña, 15192 A Coruña, SPAIN
e-mail: mosqueira@iccp.udc.es, web: http://caminos.udc.es/gmni

Key words: Smooth Particle Hydrodynamics, Meshless Methods, Free Surface Flow

Abstract
In this paper, we study different SPH formulations proposed to solve free surface problems. We center our attention in the corrections added to the SPH method in order to increase its accuracy and to improve its numerical behaviour. For this reason, we present three approaches called standard SPH, corrected SPH and standard-corrected SPH. We compare them using a simple test where we study the evolution of an elliptical water bubble. Furthermore, we also analyze the results obtained in more complex situations related with “breaking dam” problems. This kind of examples allows to check the good behaviour of these techniques.

1 Introduction

The resolution of many problems related with large deformations, complex domains, etc, takes up a high computational effort if the classical numerical techniques (finite elements, finite differences, etc) are used. For this reason, in last years other methods have been proposed. One of them are the so-called "meshless methods". Its main feature is to avoid the rigid connectivity needed in other usual numerical formulations to discretize the integration domain of the problem.

The first meshless method appeared in the 70's and it was called SPH (Smooth Particle Hydrodynamics) [1]. First of all, it was applied to astrophysics problems. But nowadays it have been applied to electromagnetism and fluid problems, because of its versatility and good numerical behaviour.

In the field of the fluid mechanics, the SPH lets to follow in time the motion of a discrete number of particles of a fluid [1]. For this reason, the linear and angular momentum preserving properties of SPH formulations is the central issue. Regarding this subject, some corrections in the kernels and in the gradient evaluation have been introduced. These improvements allow to achieve good results for example in free surface flows [3, 4].

Taking into account all of this, the objectives of this paper are the following. First, we study some SPH formulations and the differents corrections applied. We have considered three methods: the standard SPH, the corrected SPH and the standard-corrected SPH. By the other hand, we analyze the results obtained in some simple numerical tests and in more complex free surface problems, with special emphasis in "breaking dam" problems.

2 Physical aspects of the problem

The objective of the problems we want to solve is to obtain the position of any fluid particle $\boldsymbol{x}$ at any time t. We consider compressible, newtonian and isentropic fluids. So, the momentum equation, the continuity equation and the position equation can be grouped in the next system of three differential equations:

$$\frac{d\boldsymbol{a}}{dt} = \boldsymbol{F}(\boldsymbol{a}); \qquad \boldsymbol{a}^t = (\boldsymbol{v}, \boldsymbol{x}, \rho); \qquad \boldsymbol{F}(\boldsymbol{a}) = \begin{bmatrix} \boldsymbol{f} + \frac{1}{\rho}\nabla \cdot \boldsymbol{T} \\ \boldsymbol{v} \\ -\rho \nabla \cdot \boldsymbol{v} \end{bmatrix} \tag{1}$$

In this expression $\rho(\boldsymbol{x}, t)$ is the fluid density and $\boldsymbol{v}(\boldsymbol{x}, t)$ its velocity; $\boldsymbol{f}$ are the external forces by unity mass and $\nabla \cdot \boldsymbol{T}$ the internal forces by unity volume. $\boldsymbol{T}$ is the Cauchy Tensor and can be calculated using the next constitutive equation:

$$\boldsymbol{T} = -p\boldsymbol{I} + 2\mu\left(\boldsymbol{D} - \frac{1}{3}tr(\boldsymbol{D})\boldsymbol{I}\right); \qquad \boldsymbol{D} = \frac{1}{2}(\nabla \boldsymbol{v} + \nabla \boldsymbol{v}^t), \tag{2}$$

being μ the fluid viscosity, $\boldsymbol{I}$ is the second order identity tensor and p is a stress scalar field that can be evaluated using the thermodynamics expression:

$$\frac{p}{p_o} = (k+1)\left(\frac{\rho}{\rho_o}\right)^{\gamma} - k, \tag{3}$$

where k and γ are adimensional parameters and p_o and ρ_o are the atmosferical standard values [5, 6]. Using these parameters, the sound velocity can be defined as $c = \sqrt{\gamma k/\rho}$ [1].

In next sections we will see how to approximate equation (1) in a numerical way.

3 Weighted residual formulation: a Point Collocation approach

A variational form of equation (1) can be written as:

$$\int_\Omega \left\{ \frac{d\boldsymbol{a}}{dt} - \boldsymbol{F}(\boldsymbol{a}) \right\} \omega d\Omega = 0 \tag{4}$$

In order to obtain a numerical approach to expression (4), we choose nc points in Ω, called collocation points ($\boldsymbol{x}_{i_c}$), and we apply a point collocation scheme. Thus the weighting function ω is given by $\omega = \delta(\boldsymbol{x} - \boldsymbol{x}_{i_c})$, being δ the Dirac delta function. Therefore, equation (4) can be written as:

$$\frac{d\boldsymbol{a}}{dt}\Big|_{\boldsymbol{x}_{ic}} - \boldsymbol{F}(\boldsymbol{a})\Big|_{\boldsymbol{x}_{i_c}} = 0; \qquad i_c = 1, ..., n_c \tag{5}$$

In the next section we will approximate $F(\boldsymbol{a})$ in the space using the SPH method and then we will solve the resulting equation in the temporal coordinate.

4 Functional interpolation: the SPH method

A SPH approximation can be understood as a smoothing interpolation technique in which the estimated value $u_h(\boldsymbol{x})$ of a function $u(\boldsymbol{x})$ at a point $\boldsymbol{x}$ is obtained by using its values at a set of disordered points of a certain domain Ω, weighted by a kernel function $K(\boldsymbol{x}, \boldsymbol{r})$ in the next way [7]:

$$u(\boldsymbol{x}) \approx u^h(\boldsymbol{x}) = \int_{\boldsymbol{r}\in\Omega} K(\boldsymbol{x}, \boldsymbol{r}) u(\boldsymbol{r}) d\Omega \tag{6}$$

It is obvious that the weighting function plays a role of fundamental importance. Furthermore, it is the responsible for the local character of the approximation. One of the options to enforce this, is to define the weighting function so that it takes its maximum value at the point $\boldsymbol{x}$, while the information of any other point is weighted according to their distance to $\boldsymbol{x}$. Then, if the weighting function vanish outside a certain surrounding region, the approximation will have the desired local character. For example:

$$K(\boldsymbol{x}, \boldsymbol{r}) = \begin{cases} H(z)\Big|_{z=|(\boldsymbol{x}-\boldsymbol{r})/h|} > 0, & \text{if } \boldsymbol{r} \in B(\boldsymbol{x}); \\ 0, & \text{in any other point.} \end{cases} \tag{7}$$

being $H(z)$ an adequate function, such as a gaussian function, a cubic spline or any other function with similar characteristics [9]. $B(\boldsymbol{x})$ is a selected suitable subdomain in the neighbourhood of the given point $\boldsymbol{x}$, for instance

$$B(\boldsymbol{x}) = \{\boldsymbol{r} \in \Omega \ / \ |\boldsymbol{r} - \boldsymbol{x}| \leq 2h\} \tag{8}$$

The so-called dilation parameter ρ plays a very important role in (7), since it contributes to characterize the support of the weighting function.

On the other hand, the kernel $K(\boldsymbol{x}, \boldsymbol{r})$ must verify the consistency requirements, which depend on the highest order of the polynomial that must be exactly represented by the approximation.

In order to achive this, the weighting function must satisfy that [13]:

$$\int_{\boldsymbol{r}\in\Omega} K(\boldsymbol{x}, \boldsymbol{r}) d\Omega = 1; \tag{9}$$

$$\int_{\boldsymbol{r}\in\Omega} K(\boldsymbol{x},\boldsymbol{r})d^q u(\boldsymbol{x})(\boldsymbol{r}-\boldsymbol{x})d\Omega = 0; \quad q = 1, ..., m \tag{10}$$

An example of weighting function with lineal consistency is the cubic spline [13].

Now it is necessary to explain how to construct the discrete form, i.e., how to calculate the previous integrals in a numerical way

$$u^h(\boldsymbol{x}) \;=\; \int_{\boldsymbol{r}\in\Omega} K(\boldsymbol{x},\boldsymbol{r})u(\boldsymbol{r})d\Omega \simeq \sum_{i_p=1}^{n_p} V(\boldsymbol{r}_{i_p})K(\boldsymbol{x},\boldsymbol{r}_{i_p})u(\boldsymbol{r}_{i_p}) = \widehat{u}^h(\boldsymbol{x}). \tag{11}$$

being $\boldsymbol{r}_{i_p}$ the integration points, $V(\boldsymbol{r}_{i_p})$ the integration weighting functions and n_p the total number of non-structured integration points in Ω. In this paper, these integration points are also called nodal points.

The new difficult in the discrete case is that the consistency conditions in (10) are not verify. For this reason, some correction function $W(\boldsymbol{x},\boldsymbol{r}_{i_p})$ must be used. Therefore, equation (11) must be written in the next way:

$$\widehat{u}^h(\boldsymbol{x}) \;=\; \sum_{i_p=1}^{n_p} V(\boldsymbol{r}_{i_p})W(\boldsymbol{x},\boldsymbol{r}_{i_p})K(\boldsymbol{x},\boldsymbol{r}_{i_p})u(\boldsymbol{r}_{i_p}) \tag{12}$$

4.1 Kernel correction

The objective of the kernel correction is to achieve a discrete approximation with consistency order m. For example, we can choose the next $W(\boldsymbol{x},\boldsymbol{r})$ correction function [13]

$$W(\boldsymbol{x},\boldsymbol{r}) = \boldsymbol{p}^t(\boldsymbol{x}) < \boldsymbol{p},\boldsymbol{p}^t >_K^{-1} \boldsymbol{p}(\boldsymbol{r}) \Rightarrow K^*_m(\boldsymbol{x},\boldsymbol{r}) = \boldsymbol{p}^t(\boldsymbol{x}) < \boldsymbol{p},\boldsymbol{p}^t >_K^{-1} \boldsymbol{p}(\boldsymbol{r})K(\boldsymbol{x},\boldsymbol{r}), \tag{13}$$

where

$$\boldsymbol{p}(\boldsymbol{r}) = \boldsymbol{\varphi}(\boldsymbol{z})\Big|_{\boldsymbol{z}=(\boldsymbol{r}-\boldsymbol{x})/h}, \tag{14}$$

being $\boldsymbol{\varphi}(\boldsymbol{z})$ the selected polinomial base and $K^*(\boldsymbol{x},\boldsymbol{r})$ the corrected kernel. The scalar product can be calculated using:

$$< f, g >_K = \sum_{ip=1}^{np} V(\boldsymbol{r}_{ip})K(\boldsymbol{x},\boldsymbol{r}_{ip})f(\boldsymbol{r}_{ip})g(\boldsymbol{r}_{ip}), \tag{15}$$

and the function approximation $u(\boldsymbol{x})$ can be written as:

$$\widehat{u}^h(\boldsymbol{x}) \;=\; \boldsymbol{p}^t(\boldsymbol{x}) < \boldsymbol{p},\boldsymbol{p}^t >_K^{-1} < \boldsymbol{p}, u >_K, \tag{16}$$

In the physical problems we solve, it is necessary to approximate the gradient of some functions. The first alternative we show is to calculate the gradient of expression (16).

4.2 Gradient correction

The gradient approximation can also be evaluated by correcting the gradient in a direct way. There are different alternatives. For example, if we define the scalar product as [13]

$$< f, g >_1 = \sum_{ip=1}^{np} V(\boldsymbol{r}_{ip})f(\boldsymbol{r}_{ip})g(\boldsymbol{r}_{ip}), \tag{17}$$

the correction function $\widehat{\boldsymbol{W}}$ can be calculated as

$$\widehat{\boldsymbol{W}} =< \nabla K_0^*, (\boldsymbol{x}-\boldsymbol{r})^t >_1^{-1}; \tag{18}$$

being $\nabla K_0^*(\boldsymbol{x},\boldsymbol{r})$ the gradient of a zero-order corrected kernel:

$$\nabla K_0^*(\boldsymbol{x},\boldsymbol{r}) = \nabla < 1,1 >_K^{-1} K(\boldsymbol{x},\boldsymbol{r}) + < 1,1 >_K^{-1} \nabla K(\boldsymbol{x},\boldsymbol{r}) \tag{19}$$

Therefore, the so-called one-order mixed kernel-gradient correction is:

$$\nabla_1^* K_0^*(\boldsymbol{x},\boldsymbol{r}) =< \nabla K_0^*, (\boldsymbol{x}-\boldsymbol{r})^t >_1^{-1} \nabla K_0^*(\boldsymbol{x},\boldsymbol{r}) \tag{20}$$

and the gradient approximation:

$$\nabla^h u(\boldsymbol{x}) =< \nabla_1^* K_0^*, u >_1 \tag{21}$$

5 Spatial discretization schemes

In this section we applied the studied interpolation techniques in order to solve equation (1). We use three different discretization schemes.

Firstly, we approach the so-called standard SPH method, that is, the SPH method without any correction. Therefore, the consistency conditions are not verify. Furthermore, it is considered a non viscous fluid but it is introduced an artificial viscosity.

In second place, we approach the corrected SPH method. In this case, the kernel correction is applied to approximate any function and the mixed kernel-gradient correction is applied to approximate its gradient. In order to preserve linear momentum and angular momentum it is necessary to use a zero-order correction and a one-order gradient correction. Furthermore, in this case it is considered a viscous fluid.

Finally, we propose a new formulation. We have called it standard-corrected SPH method. The objective of this approach is to analyze how the corrections and the use of an artificial viscosity affect the results obtained.

In all the cases, the integration weights are calculated using the volume associated to each particle. That is, if the mass of each particle is called m_j, its coordinates $\boldsymbol{r}_j$ and its density ρ_j, this integration weights are: $V(\boldsymbol{r}_j) = m_j/\rho_j$ [1].

5.1 The standard SPH method

If it is used the standard SPH method, the motion of each fluid particle $\boldsymbol{x}_i$ can be calculated by using the expression:

$$\frac{d\boldsymbol{v}(\boldsymbol{x}_i)}{dt} = \boldsymbol{f}(\boldsymbol{x}_i) + \sum_{j=1}^{n} m_j \Big(\frac{p(\boldsymbol{x}_i)}{\rho(\boldsymbol{x}_i)^2} + \frac{p(\boldsymbol{x}_j)}{\rho(\boldsymbol{x}_j)^2} + \boldsymbol{\Pi}_{i,j} \Big) \nabla_{\boldsymbol{r}} K(\boldsymbol{r}_j, \boldsymbol{x}_i) \tag{22}$$

$$\frac{d\rho(\boldsymbol{x}_i)}{dt} = -\rho(\boldsymbol{x}_i) \sum_{j=1}^{n} V(\boldsymbol{r}_j) \big(\boldsymbol{v}(\boldsymbol{r}_j) - \boldsymbol{v}(\boldsymbol{x}_i) \big)^t \cdot \nabla_{\boldsymbol{r}} K(\boldsymbol{x}_i, \boldsymbol{r}_j); \qquad \frac{d\boldsymbol{x}_i}{dt} = \boldsymbol{v}(\boldsymbol{x}_i) \tag{23}$$

It can be observed that it is considered a non viscous fluid. However an artificial viscosity has been introduced. This viscosity is defined as [14]:

$$\boldsymbol{\Pi}_{i,j} = \begin{cases} \frac{-\alpha c_{i,j} \mu_{i,j} + \beta \mu_{i,j}^2}{\rho_{i,j}}, & \text{for } \boldsymbol{v}_{i,j}^t \cdot \boldsymbol{r}_{i,j} < 0; \\ 0, & \text{in any other case,} \end{cases} \tag{24}$$

being:

$$\mu_{i,j} = \frac{h\boldsymbol{v}_{i,j}^t \cdot \boldsymbol{r}_{i,j}}{\boldsymbol{r}_{i,j}^2 + 0.01h^2}; \qquad \rho_{i,j} = \frac{1}{2}\big(\rho(\boldsymbol{x}_i) + \rho(\boldsymbol{r}_j)\big); \tag{25}$$

$$c_{i,j} = \frac{1}{2}(c_i + c_j); \qquad \boldsymbol{v}_{i,j} = \boldsymbol{v}(\boldsymbol{x}_i) - \boldsymbol{v}(\boldsymbol{r}_j); \qquad \boldsymbol{r}_{i,j} = \boldsymbol{r}_i - \boldsymbol{r}_j. \tag{26}$$

A typical value of α is $\alpha = 0.01$ and c_i is the sound velocity at $\boldsymbol{x}_i$ [1]. In problems like the one we try to solve, it is usual to take $\beta = 0$ [1].

Furthermore, in this method the velocity introduced in the continuity equation and in the equation that calculates the position of each particle are corrected in order to smooth the results obtained with the momentum equation. The next expressions are used:

$$\frac{d\boldsymbol{v}(\boldsymbol{x}_i)}{dt} = \boldsymbol{f}(\boldsymbol{x}_i) + \sum_{j=1}^{n} m_j \Big(\frac{p(\boldsymbol{x}_i)}{\rho(\boldsymbol{x}_i)^2} + \frac{p(\boldsymbol{x}_j)}{\rho(\boldsymbol{x}_j)^2} + \boldsymbol{\Pi}_{i,j} \Big) \nabla_{\boldsymbol{r}} K(\boldsymbol{r}_j, \boldsymbol{x}_i) \tag{27}$$

$$\boldsymbol{v}^*(\boldsymbol{x}_i) = \boldsymbol{v}(\boldsymbol{x}_i) + \epsilon \sum_{j=1}^{n} m_j \left(\frac{\boldsymbol{v}_{i,j}}{\rho_{i,j}} \right) K(\boldsymbol{x}_i, \boldsymbol{r}_j) \tag{28}$$

$$\frac{d\rho(\boldsymbol{x}_i)}{dt} = -\rho(\boldsymbol{x}_i) \sum_{j=1}^{n} V(\boldsymbol{r}_j) \big(\boldsymbol{v}^*(\boldsymbol{r}_j) - \boldsymbol{v}^*(\boldsymbol{x}_i)\big)^t \cdot \nabla_{\boldsymbol{r}} K(\boldsymbol{x}_i, \boldsymbol{r}_j); \qquad \frac{d\boldsymbol{x}_i}{dt} = \boldsymbol{v}^*(\boldsymbol{x}_i) \tag{29}$$

This correction is called XSPH and it tries to keep the particles more orderly and, in high speed flows, it prevents fluids interpenetrating. A usual value of ϵ is 0.5 [1].

5.2 The corrected SPH method

Taking into account equations (13) and (20), the motion of each fluid particle can be approximated by using the expression:

$$\frac{d\boldsymbol{v}(\boldsymbol{x}_i)}{dt} = \boldsymbol{f}(\boldsymbol{x}_i) - \frac{1}{\rho(\boldsymbol{x}_i)} \sum_{j=1}^{n} V(\boldsymbol{r}_j) \boldsymbol{T}(\boldsymbol{r}_j) \nabla^*_{\boldsymbol{r}} K^*(\boldsymbol{x}_i, \boldsymbol{r}_j); \tag{30}$$

$$\frac{d\rho(\boldsymbol{x}_i)}{dt} = \rho(\boldsymbol{x}_i) \sum_{j=1}^{n} V(\boldsymbol{r}_j) \boldsymbol{v}(\boldsymbol{r}_j)^t \cdot \nabla^*_{\boldsymbol{r}} K^*(\boldsymbol{x}_i, \boldsymbol{r}_j); \qquad \frac{d\boldsymbol{x}_i}{dt} = \boldsymbol{v}(\boldsymbol{x}_i) \tag{31}$$

being

$$\boldsymbol{T}(\boldsymbol{r}_j) = p(\boldsymbol{r}_j)\boldsymbol{I} + 2\mu \Big[\boldsymbol{D}(\boldsymbol{r}_j) - \frac{1}{3} tr\big(\boldsymbol{D}(\boldsymbol{r}_j)\big)\boldsymbol{I} \Big]; \tag{32}$$

$$\boldsymbol{D}(\boldsymbol{r}_j) = \frac{\Big(\nabla \boldsymbol{v}(\boldsymbol{r}_j) + \nabla \boldsymbol{v}(\boldsymbol{r}_j)^t\Big)}{2}; \nabla_{\boldsymbol{r}} \boldsymbol{v}(\boldsymbol{r}_j) = -\sum_{k=1}^{n} V(\boldsymbol{r}_k) \boldsymbol{v}(\boldsymbol{r}_k) \nabla^*_1 K^*_0(\boldsymbol{r}_j, \boldsymbol{r}_k) \tag{33}$$

5.3 The standard-corrected SPH method

In this third case, we use the same corrections as in the previous formulation. But now, we have replaced the natural viscosity with the artificial used in the standard SPH method. The equations we solve are:

$$\frac{d\boldsymbol{v}(\boldsymbol{x}_i)}{dt} = \boldsymbol{f}(\boldsymbol{x}_i) + \sum_{j=1}^{n} m_j \Big(\frac{p(\boldsymbol{x}_i)}{\rho(\boldsymbol{x}_i)^2} + \frac{p(\boldsymbol{x}_j)}{\rho(\boldsymbol{x}_j)^2} + \boldsymbol{\Pi}_{i,j} \Big) \nabla_1^* K_0^*(\boldsymbol{r}_j, \boldsymbol{x}_i) \tag{34}$$

$$\frac{d\rho(\boldsymbol{x}_i)}{dt} = \rho(\boldsymbol{x}_i) \sum_{j=1}^{n} V(\boldsymbol{r}_j) \boldsymbol{v}(\boldsymbol{r}_j)^t \cdot \nabla_1^* K_0^*(\boldsymbol{x}_i, \boldsymbol{r}_j); \qquad \frac{d\boldsymbol{x}_i}{dt} = \boldsymbol{v}(\boldsymbol{x}_i) \tag{35}$$

6 Time discretization

In this section a time integration scheme is approached. Many different techniques have been proposed by other authors [3, 14]. In this paper we center our attention in a one-step method. So equation (1) can be approximated in the next way:

$$\boldsymbol{u}_{i+1} = \boldsymbol{u}_i + \Delta t \Phi(\boldsymbol{x}_i, \boldsymbol{u}_i), \tag{36}$$

where $\Phi(\boldsymbol{x}_i, \boldsymbol{u}_i)$ depends on the one-step method used.

In this paper, we use a variant of the modified Euler method. We try to calculate the value of the position, the velocity and the density of each particle at a time t_{i+1} knowing its values at a time t_i. For this reason, we predict its values at a time between called $t_{i/2}$ and we correct then using now the subscript $t_{i+1/2}$. Taking all of this into account, we solve

$$\boldsymbol{v}_{i/2} = \boldsymbol{v}_i + \frac{\Delta t}{2} \Big(\frac{d\boldsymbol{v}}{dt} \Big)_{i-\frac{1}{2}}; \; \boldsymbol{x}_{i/2} = \boldsymbol{x}_i + \frac{\Delta t}{2} \boldsymbol{v}_i; \; \rho_{i/2} = \rho_i + \frac{\Delta t}{2} \Big(\frac{d\rho}{dt} \Big)_i. \tag{37}$$

$$\boldsymbol{v}_{i+\frac{1}{2}} = \boldsymbol{v}_i + \frac{\Delta t}{2} \Big(\frac{d\boldsymbol{v}}{dt} \Big)_{i/2}; \; \boldsymbol{x}_{i+\frac{1}{2}} = \boldsymbol{x}_i + \frac{\Delta t}{2} \boldsymbol{v}_{i+\frac{1}{2}}; \; \rho_{i+\frac{1}{2}} = \rho_i + \frac{\Delta t}{2} \Big(\frac{d\rho}{dt} \Big)_{i+\frac{1}{2}}. \tag{38}$$

$$\boldsymbol{v}_{i+1} = 2\boldsymbol{x}_{i+\frac{1}{2}} - \boldsymbol{x}_i; \; \boldsymbol{x}_{i+1} = 2\boldsymbol{v}_{i+\frac{1}{2}} - \boldsymbol{v}_i; \; \rho_{i+1} = 2\rho_{i+\frac{1}{2}} - \rho_i \tag{39}$$

This time integration scheme implies an explicit formulation.

7 Examples

7.1 Evolution of an elliptical water bubble

As a simple test of the three SPH formulations, we calculate the flow of an elliptical water bubble in two dimensions when the velocity field is linear in the coordinates, $\boldsymbol{v}_o = (-100x, 100y)$. The initial configuration is a unit circle. We study the two axes evolution, a and b. If the fluid remains incompressible ($ab = \text{cte} = 1$), the problem can be solved in an analytical way [1].

In figure 1 we show the results obtained using the standard SPH, the corrected SPH and the standard-corrected SPH. The parameters we use are: $\gamma = 7$, $k = 285,714\ MN/m^2$ and $\rho_o = 1000\ kg/m^3$. In figure (1a) it can be observed the initial particle configuration. In all cases, we use 1308 unstructured particles. In figure (1b) we compare the value of the product ab. It could be equals 1. The corrected SPH method and the standard-corrected method have a similar behaviour and the errors obtained are lower that those obtained with the standard SPH method.

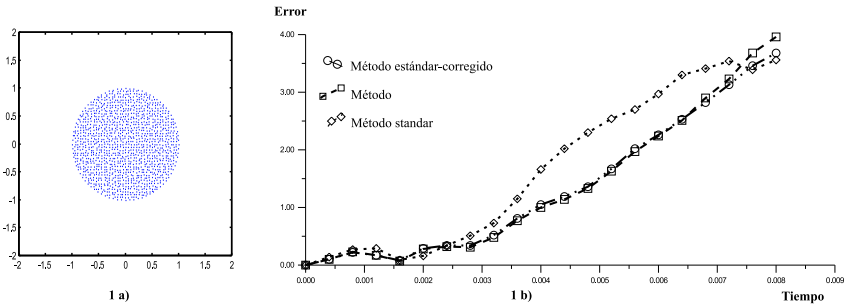

Figure 1: Initial position of the particles and numerical errors comparison.

7.2 "Breaking dam" with a slope dowstream

In this example we simulate a simplified breaking dam with a slope downstream. In this case, the external forces are the gravity. Furthermore, the boundaries determine the motion of the particles. In this paper, we consider that the boundary particles exert central forces on fluid particles. These forces are calculated using the Lennard-Jones expression, based on the forces between molecules. For a boundary and fluid particle separated by a distance $\boldsymbol{r}$ the force per unit mass $f(\boldsymbol{r})$ has the form:

$$f(\boldsymbol{r}) = \begin{cases} D\left[\left(\frac{r_0}{r}\right)^4 - \left(\frac{r_0}{r}\right)^2\right]\frac{\boldsymbol{r}}{r^2}, & \text{if } r \leq r_0; \\ 0, & \text{in other case} \end{cases} \tag{40}$$

where D (with dimension velocity squared) is a scalar factor which was chosen to be comparable to or exceed the kinetic energy per unit mass of the particles. In this case, we chose $D \approx 5gH$, being g the gravity and H the water initial height, and r_0 is chosen to be the initial particle spacing.

In figure 2, it is shown the results obtained with this method. Each graphic represents the position of all the particles at intermediate times.

8 Conclusions

In this paper, the SPH method applied to free surface problems have been studied. Three different formulations have been analyzed: the standard SPH method, the corrected SPH method and standard-corrected SPH method. In both cases, first we have approached the equations that represents the physical problem we try to solve, then we have selected the points or particles where we want to calculate the solution and, finally, we have approximated the differential equation in spacial and in time dimensions and we have replaced it by an algebraic equation. Furthermore, we have center our attention in the approach of the corrections applied to preserve linear and angular momentums.

The standard-corrected SPH method allows to analyze the influence of the corrections that have been introduced in the formulation and the importance of the viscosity terms. The conclusion is that the correction factors improve the accuracy of the results more than the use of a natural viscosity.

In the same way, the second example solved shows the good properties of these techniques to deal with free surface problems, like those called "breaking dam" problems. It could be interesting in future to compare these numerical results with some experimental tests. Moreover, this example has showed us the influence of the formulation used to approximate the boundary conditions. For this reason, we are now studing other techniques to treat with these areas of the fluids.

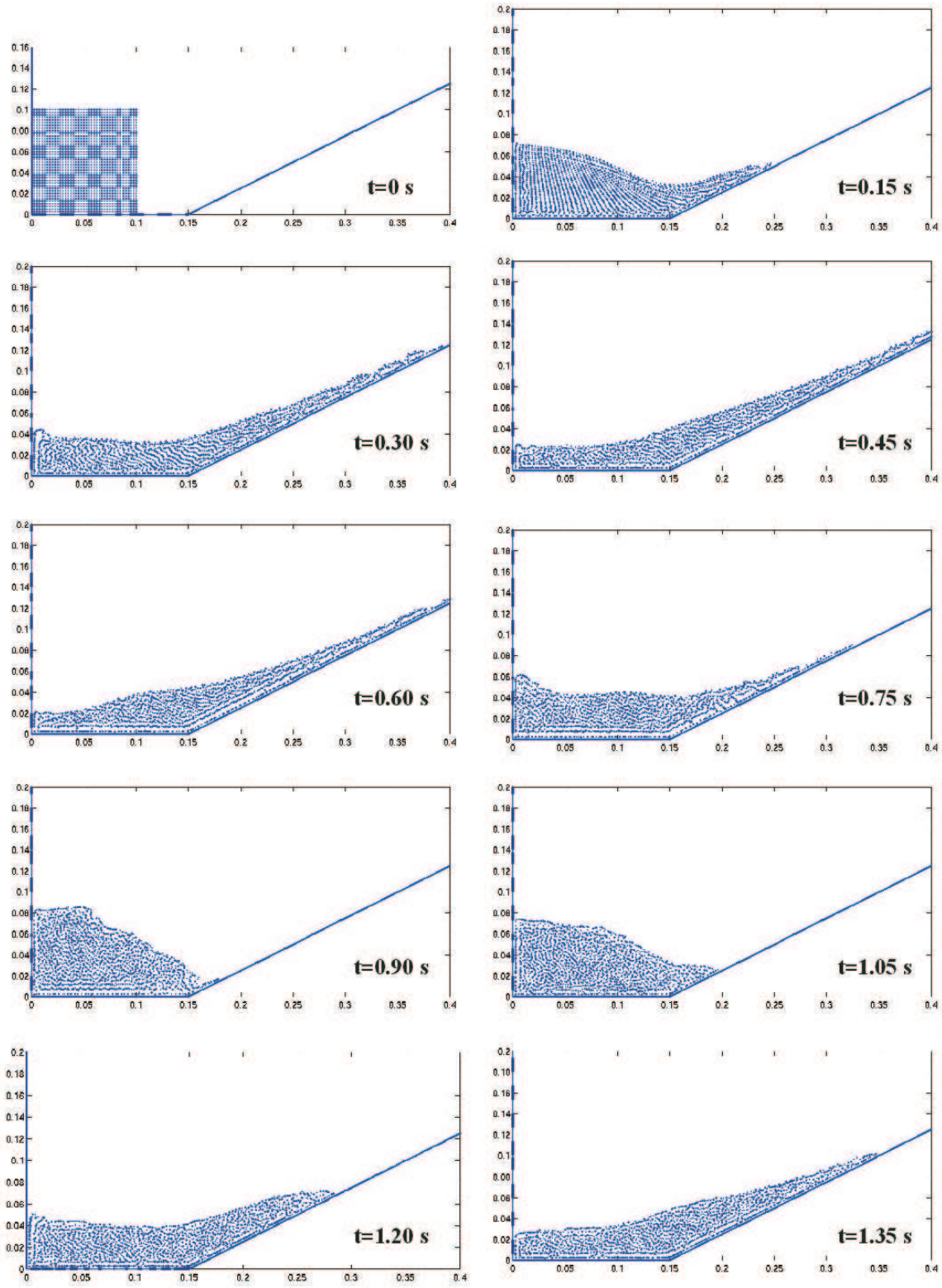

Figure 2: Time evolution of fluid particles in a “breaking dam” problem with a slope downstream

9 Acknowledgements

This work has been partially supported by the SGPICT of the "Ministerio de Ciencia y Tecnología" of the Spanish Government, cofinanced by research fellowships of the R&D Secretary of "Xunta de Galicia" and the "Universidade de A Coruña".

References

[1] J.J. Monaghan *Simulating Free Surface Flows with SPH*, Annu. Rev. Astron. Astrophys., **30**, 543-574; 1992

[2] T. Belytschko, Y. Krongauz, D. Organ, M. Fleming and P. Krysl *Meshless methods: An overview and recent developments* Comput. Methods in Appl. Mech. and Engrg., **139**,3-49; 1996

[3] J. Bonet, T.S.L. Lok *Variational and momentum preseving aspects of Smooth Particle Hydrodynamics formulations* Comput. Methods in Appl. Mech. and Engrg., **180**,97-115; 1998

[4] S. Fernández-Méndez *Mesh-Free Methods and Finite Elements: Friend or Foe?* Doctoral Thesis. Barcelona ; September 2001

[5] M.E. Gurtin *An Introduction to Continuum Mechanics* Mathematics in Science and Engineering, **158**, Academic Press; 1981

[6] F.M. White *Mecánica de fluidos* McGraw-Hill; 1983

[7] P.W. Randles, L.D. Libersky *SPH: Some recent improvements and applications* Comput. Methods in Appl. Mech. and Engrg., **139**,375-408; 1996

[8] O.C. Zienkiewicz and K. Morgan *Finite Elements and Approximation* John Wiley & Sons, Inc; 1983

[9] S. Kulasegaram *Development of Particle Based Meshless Method with Applications in Metal Forming Simulations* Doctoral Thesis. University of Wales Swansea; March 1999

[10] W. K. Liu, S. Jun & Y.F. Zhang *Reproducing Kernel Particle Methods* Int. J. Num. Meth. Engrg., **20**; 1995

[11] T. Belytschko, Y. Krongauz, J. Dolbow, and C. Gerlach *On the Completeness of Meshfree Particle Methods* Int. J. Num. Meth. Engrg., **43**,785-819; 1998

[12] G. Mosqueira, I. Colominas, J. Bonet, F. Navarrina, M. Casteleiro *Development of integration schemes for meshless numerical approaches based on the SPH method.* ECCOMAS CFD 2001, Swansea, 4-7 September 2001.

[13] L. Cueto-Felgueroso, G. Mosqueira, I. Colominas, F. Navarrina, M. Casteleiro *Análisis de formulaciones numéricas SPH para la resolución de problemas de flujo en superficie libre* Métodos Numéricos en Ingeniería V, Madrid, 4-7 June 2002.

[14] J.P. Morris *An Overview of the Method of Smoothed Particle Hydrodynamics* Universitat Kaiserslautern. Internal Report; 1995